THE JOURNAL OF PHYSICAL CHEMISTRY C

Article

pubs.acs.org/JPCC

Aqueous NMR Signal Enhancement by Reversible Exchange in a Single Step Using Water-Soluble Catalysts

Fan Shi,[†,∇,¶] Ping He,[†,○,¶] Quinn A. Best,[†,◆] Kirsten Groome,[†] Milton L. Truong,[§] Aaron M. Coffey,[§] Greg Zimay,[†] Roman V. Shchepin,[§] Kevin W. Waddell,[§] Eduard Y. Chekmenev,[§,∥,⊥,#] and Boyd M. Goodson*[,†,‡]

[†]Department of Chemistry and Biochemistry, and [‡]Materials Technology Center, Southern Illinois University, Carbondale, Illinois 62901, United States

[§]Department of Radiology, Vanderbilt University Institute of Imaging Science, Nashville, Tennessee 37232, United States

[∥]Department of Biomedical Engineering, Vanderbilt University, Nashville, Tennessee 37235, United States

[⊥]Vanderbilt-Ingram Cancer Center, Nashville, Tennessee 37232, United States

[#]Russian Academy of Sciences, Leninskiy Prospekt 14, Moscow, 119991, Russia

Supporting Information

ABSTRACT: Two synthetic strategies are investigated for the preparation of water-soluble iridium-based catalysts for NMR signal amplification by reversible exchange (SABRE). In one approach, PEGylation of a variant *N*-heterocyclic carbene provided a novel catalyst with excellent water solubility. However, while SABRE-active in ethanol solutions, the catalyst lost activity in >50% water. In a second approach, synthesis of a novel di-iridium complex precursor where the cyclooctadiene (COD) rings have been replaced by CODDA (1,2-dihydroxy-3,7-cyclooctadiene) leads to the creation of a catalyst [IrCl(CODDA)IMes] that can be dissolved and activated in water—enabling aqueous SABRE in a single step, without need for either an organic cosolvent or solvent removal followed by aqueous reconstitution. The potential utility of the CODDA catalyst for aqueous SABRE is demonstrated with the ∼(−)32-fold enhancement of ^{1}H signals of pyridine in water with only 1 atm of parahydrogen.

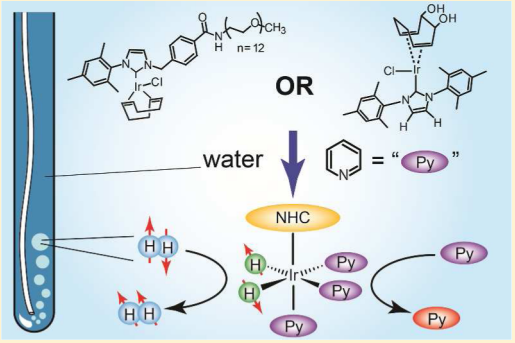

INTRODUCTION

Because of their inherent advantages (including high spatiotemporal resolution, lack of ionizing radiation, and the ability to spectrally distinguish multiple signal sources), magnetic resonance imaging (MRI)-based molecular imaging[1,2] techniques promise to revolutionize clinical imaging—from the screening and diagnosis of disease, to the assessment of treatment response. However, the inherently low detection sensitivity of conventional magnetic resonance techniques makes it challenging to detect and track low-concentration species in vivo, such as gas species in lung spaces or metabolic biomarkers in blood or other tissues. Hyperpolarization[3] techniques like dissolution dynamic nuclear polarization (d-DNP),[4,5] spin-exchange optical pumping (SEOP),[6,7] and parahydrogen induced polarization (PHIP)[8,9] offer the possibility of overcoming the problem of low agent concentration by increasing the nuclear spin polarization—and hence MR signal—by several orders of magnitude.

Signal amplification by reversible exchange (SABRE)[10] is a relatively new hyperpolarization technique pioneered by Duckett, Green, and co-workers in 2009.[11,12] In SABRE, an organometallic catalyst is used to colocate a molecular substrate to be hyperpolarized and parahydrogen (pH_2)—a source of pure nuclear spin order. Like traditional PHIP,[8,9,13−19] SABRE is of interest because it is cost-effective, potentially continuous, scalable, and rapid (achieving polarization enhancement in seconds).[10−12,20−40] However, unlike traditional PHIP, SABRE does not require permanent alteration of the substrate to hyperpolarize it.[11] Since its inception, considerable effort has been put forth to broaden the applicability of SABRE by investigating alternative catalyst structures,[21,28,41−45] improving the nuclear spin polarization achieved for protons[34,46] and various heteronuclei[30,32,47−50] (including through the application of variable applied DC and AC fields), demonstrating high-resolution imaging[25,50] (including at low magnetic field[51]), widening the range of amenable substrate types,[36] achieving enhancement in the limits of both low-[29,52] and high-concentration[49] agents (including in complex mixtures[20]), and demonstrating SABRE with (and separation/reuse of) heterogeneous microscale/nanoscale catalysts.[53,54]

Other efforts have concerned the extension of SABRE to aqueous environments. Because of the poor aqueous solubility

Received: May 4, 2016
Revised: May 11, 2016
Published: May 11, 2016

DOI: 10.1021/acs.jpcc.6b04484
J. Phys. Chem. C 2016, 120, 12149−12156

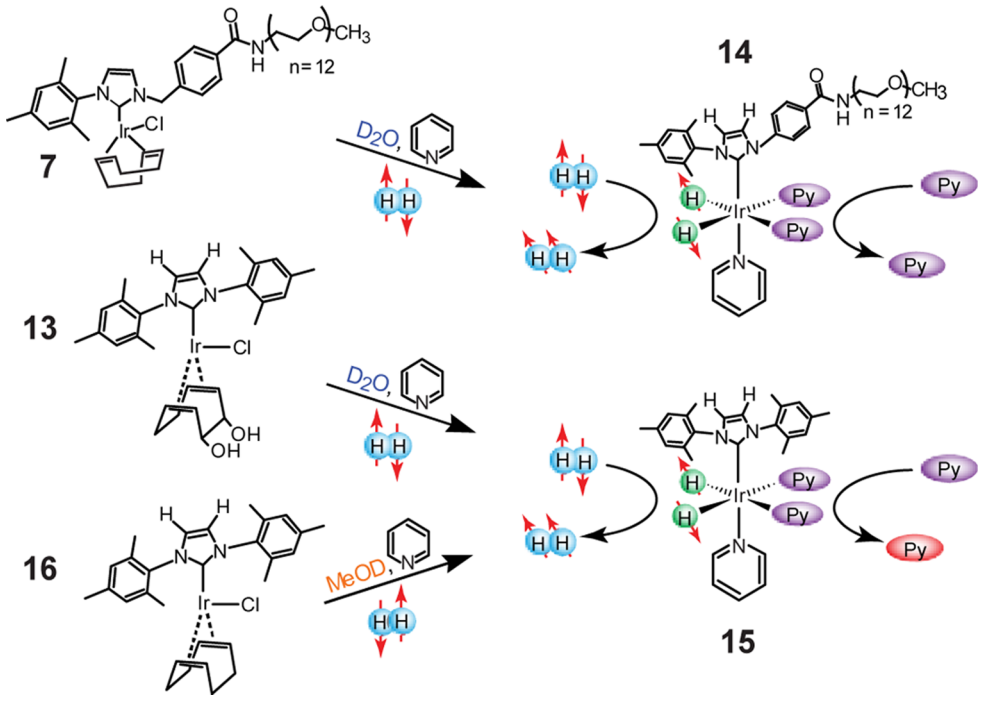

Figure 1. Relevant structures for studying SABRE in aqueous environments in the present work, pre (**7**, **13**, and **16**) and post (**14** and **15**) activation in the presence of H_2 gas and pyridine (py) substrate. **16** is the "traditional" Ir/IMes SABRE catalyst in its preactivated form, whereas **7** and **13** are the water-soluble PEGylated and cyclooctadiene-diol ("CODDA") variants, respectively (the numbering of the above structures is explained in the Supporting Information Figures S1 and S2, which, respectively, summarize the synthesis of structures **7** and **13**).

of the "standard" SABRE catalyst ([IrCl(COD) (IMes)],[46,55,56] where "COD" = cyclooctadiene and "IMes" = 1,3-bis(2,4,6-trimethylphenyl)imidazol-2-ylidene), recent promising efforts have relied on organic cosolvents to achieve SABRE in aqueous/organic mixtures[34,45,50,57] However, in other previous work we recently found that the chemical changes that accompany this catalyst's activation also endow it with water solubility;[57] following activation, the organic solvent may be completely removed and the activated catalyst can be subsequently reconstituted in deuterated water to achieve SABRE enhancement.

Here we report our efforts to develop novel homogeneous catalysts that may lead to improved SABRE in aqueous environments, without the need for separate catalyst activation, organic solvent removal, or subsequent aqueous reconstitution.[58,59] Two different strategies were utilized to alter the structure—and hence aqueous solubility—of the original standard catalyst by targeting either the *N*-heterocyclic carbene moiety or the COD group, respectively (Figure 1). For the former, PEGylation[60] of a variant of the aromatic carbene moiety provided much greater aqueous solubility for the catalyst ("**7**"); however, while that catalyst is SABRE-active in ethanol solutions, it lost activity in >50% water. For the latter, synthesis of a di-iridium complex precursor where the COD rings have been replaced by CODDA (1,2-dihydroxy-3,7-cyclooctadiene) permits creation of a catalyst [IrCl(CODDA)-IMes] ("**13**") that can be dissolved and activated in water, enabling aqueous SABRE in a single step without need for any organic cosolvent. The potential utility of the CODDA catalyst for aqueous SABRE is demonstrated with the ∼(−)32-fold enhancement of ^{1}H signals of pyridine in water with only 1 atm of pH_2. Taken together, these results aid the evaluation of different synthetic approaches for aqueous SABRE that, when improved and combined with other approaches, should help enable a wide range of biological, biomedical, and in vivo spectroscopic and imaging experiments.

RESULTS AND DISCUSSION

Exploring SABRE with the PEGylated Catalyst. The PEGylated catalyst **7** was examined to determine its efficacy for SABRE in organic and aqueous environments. SABRE experiments were performed by bubbling pH_2 thoroughly into the NMR tube while located outside of the magnet ("low-field"), followed by immediate transfer of the sample into the 9.4 T NMR magnet for "high-field" detection of enhanced ^{1}H NMR spectra. The catalyst was activated via pH_2 bubbling in the presence of excess substrate prior to use in SABRE experiments, and the low mixing field was somewhat variable (∼11 ± 5 mT) and was not systematically optimized. Enhancements were recorded for the test substrate pyridine (py); results for all of the experiments described in this work are summarized in Table 1.

In an early set of experiments (not shown), bubbling pH_2 at atmospheric pressure gave up to ∼16-fold enhancements for the ^{1}H NMR signals of py in 100% d_6-ethanol. The addition of D_2O to d_4-methanol solutions had lower enhancements than d_6-ethanol, with ∼20% D_2O/∼80% d_4-methanol yielding only ∼6-fold ^{1}H signal enhancements. Higher volume fractions (e.g., 50/50) of D_2O in d_4-methanol resulted in no observable SABRE enhancements under these conditions.

The lower SABRE enhancements in solutions with increasing water fractions were originally rationalized by the ∼15-fold lower solubility of H_2 gas in water compared to that in alcohol-based solvents.[61] To mitigate the H_2 solubility limitation of aqueous solutions, the apparatus was altered to allow pH_2 pressures of up to ∼60 psi positive pressure (∼5.1 atm total H_2 pressure). Bubbling pH_2 at 60 psi into a sample containing 100% d_6-ethanol, ∼3.5 mM of the catalyst **7**, and 35 mM py

DOI: 10.1021/acs.jpcc.6b04484
J. Phys. Chem. C 2016, 120, 12149−12156

Table 1. Polarization Enhancement (ε) Values for Three Aromatic Proton Sites of Pyridine Observed with Different Catalysts in Aqueous and Nonaqueous Environments[a]

catalyst	solvent	ε (H_o)	ε (H_p)	ε (H_m)
7	100% d_6-ethanol	−42	−57	−11
7	100% d_6-ethanol	−45	−61	−11
7	13% D_2O/87% d_6-ethanol	−37	−27	−12
7	13% D_2O/87% d_6-ethanol	−38	−31	−14
7	43% D_2O/57% d_6-ethanol	−9.5	−5.7	−1.3
7	43% D_2O/57% d_6-ethanol	−7.3	−4.9	−0.4
7	63% D_2O/37% d_6-ethanol	∼0	∼0	∼0
13	100% D_2O	−25	−19	−11
13	100% D_2O	−32	−25	−16
16	100% D_2O	∼0	∼0	∼0

[a]Reported ε values are calculated from spectral integrals and are approximate, with estimated uncertainties of ∼10%. Results from the top two acquisitions for each condition are reported.

gave rise to ∼40−60-fold enhancement of the ^{1}H NMR signal from the substrate (e.g., Figure 2b) compared to the signal acquired at thermal equilibrium (Figure 2a; the conventional SABRE catalyst **16** is also effective in 100% d_6-ethanol[57]). Little dependence on temperature was observed, with similar enhancements attained when the temperature was raised from 301 to 321 K.

Next, no SABRE enhancement was observed when pH_2 was bubbled in at high field (9.39 T; Figure 2, parts c and d), unlike the case with the "standard" NHC-Ir catalyst, **16**.[24,57] Also unlike the case with **16**, no strong, purely absorptive signal at ∼(−)22.8 ppm is observed from magnetically equivalent hyperpolarized hydride spins on the activated catalyst structure. Instead, the hydride region exhibits two relatively weak dispersive doublets at ca. −22.2 and ∼−23.1 ppm. These dispersive signals are reminiscent of the enhanced hydride resonances from organometallic catalysts explored previously with PHIP (e.g., $RhH_2(PPh_3)_3Cl$[13]) and, thus, are tentatively assigned to the two hydride sites on the activated catalyst (**14**) rendered effectively inequivalent by the broken symmetry of the PEGylated *N*-heterocyclic carbene. A pair of additional, much weaker dispersive signals (at ca. −22.6 and −25.9 ppm) likely arise from inequivalent hydride sites on a similar structure to **14** originating from a different chemical pathway. The absence of a high-field SABRE effect is likely a combination of inefficient conversion of spin order from pH_2 at high field and the lack of strong *z*-magnetization of the hydride spins, and is consistent with the current picture for the high-field SABRE

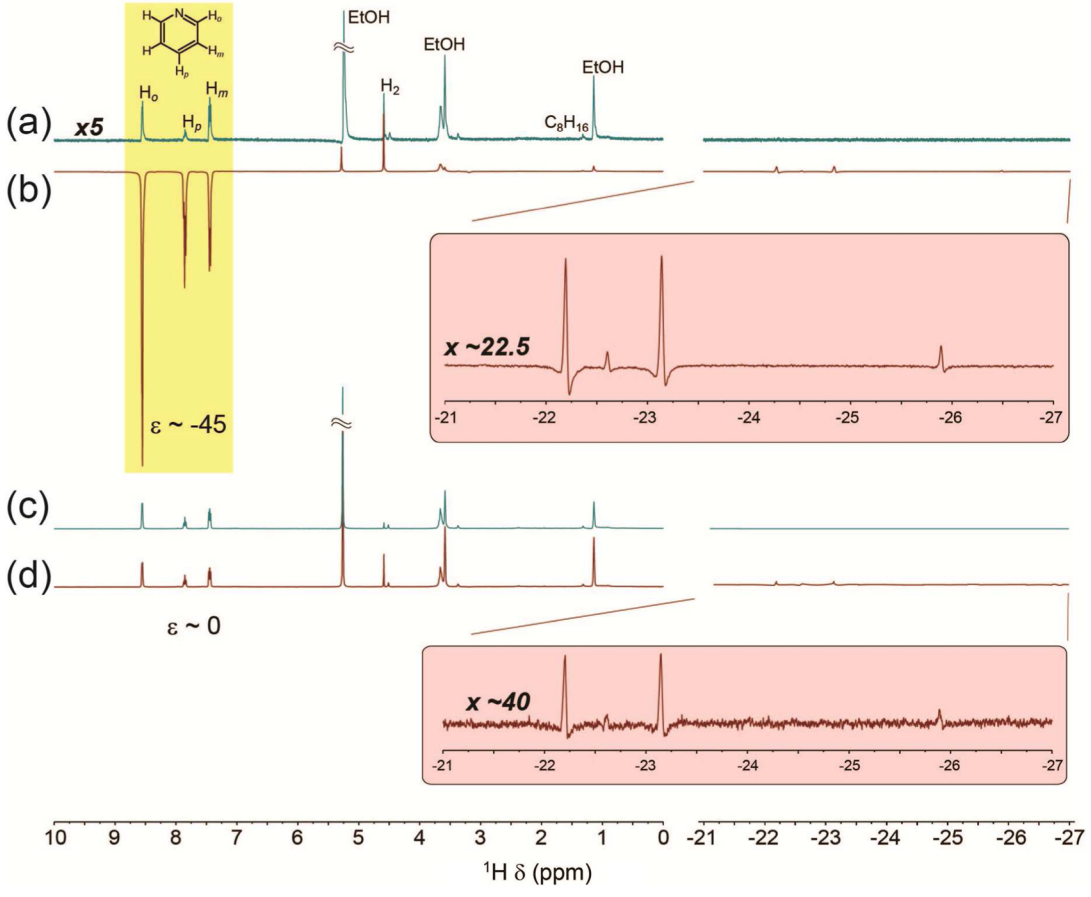

Figure 2. SABRE studies with the PEGylated Ir catalyst (**7**/**14**) in 100% deuterated ethanol. (a) Thermally polarized reference ^{1}H NMR scan from the solution following activation with pH_2 in the presence of excess substrate (py); the spectrum is vertically scaled 5-fold compared to panel b, which shows the successful observation of SABRE enhancement after 1 min of bubbling with ∼5.1 atm of pH_2 at ∼11 mT, then transfer to 9.39 T for high-field acquisition; enhancements up to ∼40−60-fold were observed with 3.5 mM catalyst and the given conditions. Panels c and d show spectra from a separate experiment, where no high-field SABRE effect was observed, i.e., where pH_2 bubbling/SABRE mixing was performed entirely at 9.39 T (d), compared to a corresponding thermally polarized spectrum (c). (Vertical scale for panels c and d is different from that of panels a and b.) Insets show amplified hydride regions from spectra in panels b and d, respectively.

DOI: 10.1021/acs.jpcc.6b04484
J. Phys. Chem. C 2016, 120, 12149−12156

mechanism—cross-relaxation akin to the spin-polarization induced nuclear Overhauser effect.[24,57,62,63]

As shown in Figure 3, parts a and b, modest aqueous fractions (~13% v/v) had only a minor negative effect on

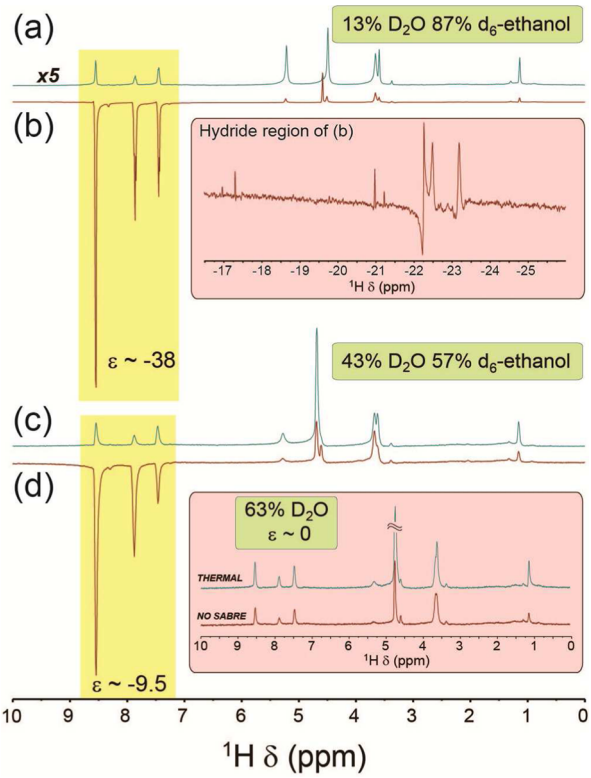

Figure 3. SABRE studies with the PEGylated Ir catalyst (**7**/**14**) in various deuterated ethanol/water mixtures. (a) Thermally polarized reference ^{1}H NMR scan from a D_2O/d_6-ethanol (~13%/87% v/v) solution following activation; the spectrum is vertically scaled 5-fold compared to panel b, which shows the successful observation of SABRE enhancement of substrate (py) ^{1}H resonances after 1 min of bubbling with 5.1 atm of pH_2 at ~11 mT, then transfer to 9.39 T for high-field acquisition; enhancements up to ~40-fold were observed with 3.5 mM catalyst and the given conditions. Changing the D_2O/d_6-ethanol fraction to ~43%/57% v/v (c and d) and 63%/37% v/v (inset) significantly impacted the magnitude of the SABRE enhancement; the SABRE spectrum in panel d showed less than an ~10-fold enhancement compared to the corresponding thermal spectrum (c), and no observed SABRE enhancement was observed in the 63%/37% solution.

SABRE enhancement (maximum $|\varepsilon|$ ~ 40). Here, the concentration of D_2O is already orders of magnitude higher than the concentrations of the catalyst and substrate. Bringing the water fraction to nearly 1:1 dropped the SABRE enhancement by ~5-fold (Figure 3, parts c and d); this observation is in reasonable agreement with the ~15-fold lower solubility of H_2 in water versus alcohol-based solvents.[61] However, higher mole fractions of water (e.g., Figure 3d, inset) have not yielded observable enhancements to date. While this second set of experiments represents a marked improvement over the first in terms of both larger enhancements and larger aqueous fractions for the solvent, the origin of the absence of SABRE at higher aqueous fractions remains unclear. One hint may lie in the changes to the hydride region of the spectrum. For example, while the primary dispersive resonances at ca. −22.2 and ~−23.1 ppm remain in the spectrum from the ~13% v/v solution (Figure 3b, inset), overall the hydride signal is attenuated, there appears to be a new absorptive resonance at ~(−)22.5 ppm, and the other weak resonances appear to have bifurcated and shifted several parts per million downfield. With ~43% D_2O, only a weak dispersive resonance at ca. −22.3 ppm remains, and with higher aqueous fractions, almost no hydride signal can be detected (not shown).

The observations of reduced (or no) SABRE enhancements in large aqueous fractions are qualitatively similar to those very recently reported by Fekete et al.,[45] who investigated the use of two different synthetic approaches for generating water-soluble iridium-based SABRE catalysts (respectively featuring sulfonated phosphine groups and IMes NHC variants difunctionalized with triazole groups). For those catalysts, significant ^{1}H NMR enhancements could be observed in organic solvents, but little or no SABRE activity was observed when the aqueous fraction was too great. In that work, the absence of SABRE activity was attributed to the much lower solubility of H_2 in water compared to the organic solvents. The observations reported here could be largely explained by the reduced pH_2 concentration; however, other effects may be contributing given the complete lack of SABRE activity with high water fractions, as well as the changes in the hydride spectra. As an aside, the solvent environment during activation (i.e., organic vs aqueous) did not affect the results. Thus, the reduced pH_2 concentration, possibly combined with structural changes of the catalyst that interfere with the formation of effective hydride species, binding of the substrate, and/or subsequent transfer of spin order from pH_2 to substrate spins, likely leads to the loss of SABRE activity with high aqueous fractions—issues that will be the subject of future study.

Exploring SABRE with the CODDA Catalyst. As mentioned above, the standard SABRE catalyst (**16**) is effectively insoluble in water for the present purposes; however, changes accompanying catalyst activation provide a water-soluble structure (e.g., **15**).[57] Thus, in light of the challenges presented by the PEGylated catalyst, an alternative design approach was devised to provide a catalyst structure with improved water solubility (e.g., [IrCl(CODDA)IMes], **13**, Figure 1) that, once activated, should yield the same SABRE-active structure as **15**—with the goal of enabling aqueous SABRE in a single step without need for any organic cosolvent.

Although not as water-soluble as **7** (at least ~10 mg/mL), according to atomic absorption spectroscopy (AAS) the solubility of the CODDA catalyst (**13**) in water is ~0.2 mg/mL; thus, a saturated solution of **13** (with ~0.3 mM dissolved concentration) was prepared in deuterated water with excess py substrate (~10 mM). Bubbling with pH_2 allowed the activation of the catalyst in an aqueous environment to be monitored in situ via hyperpolarization-enhanced ^{1}H NMR (Figure 4). More specifically, spectra from the hydride region acquired during activation of **13** are shown in Figure 4a, and these results are compared with selected spectra obtained from the standard catalyst (**16**) in deuterated water (Figure 4b) and methanol solvents (Figure 4c), respectively. At first (30 s), the signals from the hydride region for **13** are dramatically different from what is observed during activation of **16**. Reflecting the different intermediate structures present, alternating absorptive/emissive (or dispersive) signals downfield of the activated catalyst's characteristic shift (−22.8 ppm) are virtually absent, and instead the early spectra are dominated by a number of purely absorptive peaks that are mostly further upfield (i.e., with a more negative chemical shift), including a strong peak at

DOI: 10.1021/acs.jpcc.6b04484
J. Phys. Chem. C 2016, 120, 12149−12156

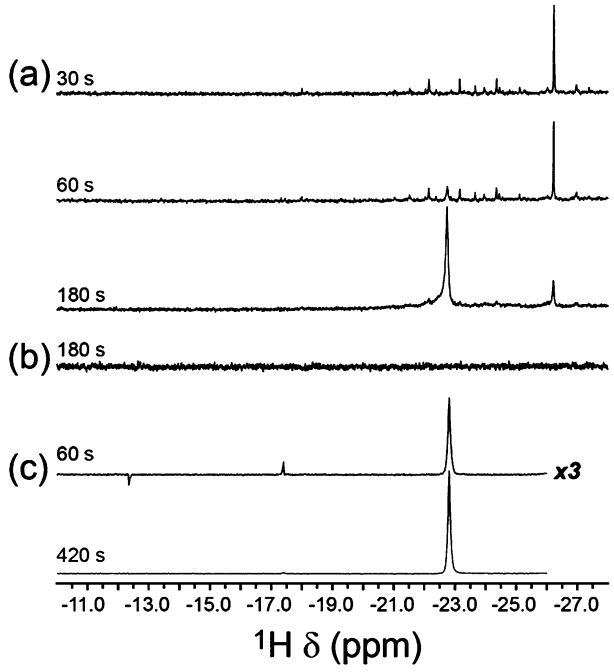

Figure 4. Comparison of the hydride regions of ^{1}H NMR spectra acquired during activation of the water-soluble CODDA/Ir SABRE catalyst **13** (a) and the conventional Ir/IMes SABRE catalyst **16** (b and c). (a) Upfield ^{1}H NMR region showing changes to the hydride resonances during activation of **13** in D_2O observed at 30, 60, and 180 s after pH_2 bubbling began (1 atm). A corresponding attempt to observe activation of the (poorly water-soluble) conventional SABRE catalyst in D_2O (**16**) exhibited no hydride signal (b). Selected spectra obtained separately during activation of **16** in deuterated methanol are shown in panel c, respectively, 60 and 420 s following the onset of pH_2 bubbling. As expected, activation of both **13** and **16** trend toward the same final hydride signal (i.e., a strong singlet at ~22.8 ppm). Spectra in panels a–c possess different vertical scales.

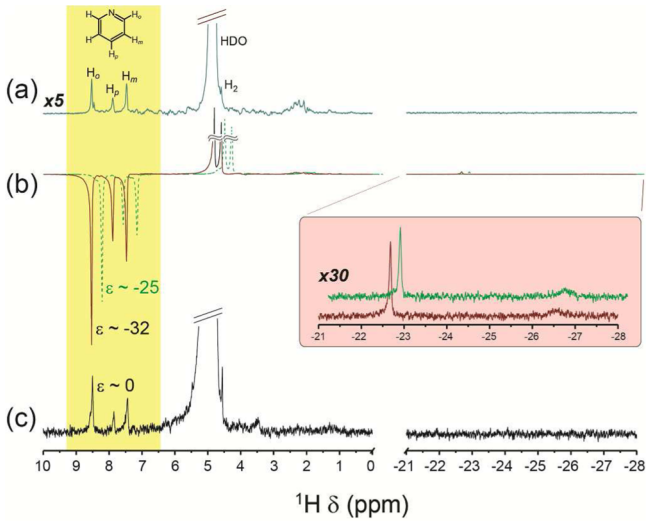

Figure 5. SABRE studies with the water-soluble CODDA/Ir SABRE catalyst (**13**/**15**) in 100% D_2O. (a) Thermally polarized reference ^{1}H NMR scan from the solution following activation with pH_2 in the presence of excess substrate (py); the spectrum is vertically scaled 5-fold compared to panel b, which shows two spectra exhibiting successful observation of SABRE enhancement after bubbling with 1 atm of pH_2 at ~10 mT [total bubbling times of 210 s (30 s immediately prior to acquisition, green dashed curve) and 240 s (30 s immediately prior to acquisition, red solid curve) for the spectra, respectively], then transfer to 9.39 T for high-field acquisition (note that the green curve is shown horizontally offset by a fraction of a ppm to show the enhancement compared to the red curve). Corresponding peak enhancements were ~25-fold and ~32-fold for py in water with only 1 atm of pH_2 bubbling in the two spectra, using a catalyst concentration of 0.3 mM. The inset shows the corresponding hydride region. A separate experiment where SABRE was attempted using the standard Ir/IMes catalyst in deuterated water exhibited no SABRE enhancement (c). (Vertical scale for panel c is different from that of panels a and b.)

−26.2 ppm from a key intermediate structure. Nevertheless, following 180 s of pH_2 bubbling, the expected singlet peak at ca. −22.8 ppm is observed, in excellent agreement with the hydride shift of the activated structure **15** obtained from the standard catalyst in methanol (Figure 4c). However, corresponding efforts to activate **16** directly in D_2O were unsuccessful, yielding a cloudy suspension and no discernible enhanced NMR signals from the hydride region (Figure 4b). In any case, the above results are consistent with successful activation of the novel catalyst **13** in water in just a few minutes to achieve the desired activated structure **15**.

Following successful activation of the CODDA catalyst in deuterated water, the potential of this catalyst for performing SABRE enhancement of ^{1}H NMR in aqueous environments was evaluated using the standard test substrate pyridine (Figure 5). With only 1 atm of pH_2 bubbling (~90% pH_2 fraction) and catalyst and substrate concentrations of ~0.3 and ~10 mM, respectively, an initial enhancement of ca. $\varepsilon = -25$ was achieved for the ortho ^{1}H py position after 30 s of bubbling at ~10 mT fringe field and subsequent transfer to 9.4 T (Figure 5b), compared to the signal from a corresponding thermal spectrum (Figure 5a). The inset of Figure 5b shows the corresponding hydride regions obtained from the CODDA catalyst during the SABRE experiments, indicating that the CODDA catalyst is essentially activated by the time the SABRE spectra were recorded (total pH_2 bubbling time of 210 and 240 s, respectively). Repeating the experiment permitted enhancements as large as ca. −32, −25, and −16 for ortho, para, and meta ^{1}H Py positions to be observed, Figure 5b; Table 1. However, the sample from Figure 4b containing an aqueous suspension of the traditional SABRE catalyst (**16**) yields no SABRE enhancement, Figure 5c.

The experiments described above were performed in deuterated water to facilitate spectral interpretation and quantification; however, this practice poses no impediment to broader application of the approach (including for ultimate in vivo experiments) because SABRE hyperpolarization generally works as well (or better) in protonated solution environments, particularly for heteronuclei.[49,64,65] We also note that these results are similar to what has been achieved using the conventional catalyst following dissolution and activation in organic solvents, drying, and reconstitution in D_2O ($\varepsilon \sim 30$), using a weaker substrate (nicotinamide) but higher pH_2 pressure (~5 atm) and greater (~1:10) catalyst/substrate ratio.[57] In any case, these results indicate the successful preparation, activation, and demonstration of a catalyst capable of easily performing SABRE enhancement in aqueous environments in a single step. This approach obviates the need for either the extra steps associated with reconstitution or the exposure of sensitive biological samples to organic solvents, and thus may also help facilitate biomedical (and ultimately in vivo) applications.

DOI: 10.1021/acs.jpcc.6b04484
J. Phys. Chem. C 2016, 120, 12149−12156

CONCLUSION

In summary, two novel approaches were investigated for creating water-soluble catalysts to increase the nuclear spin polarization of substrates via SABRE. PEGylation of an asymmetric aromatic carbene ligand provided a highly water-soluble structure that yielded ~40−60-fold ^{1}H NMR enhancements in alcohol-based solvents and in lean water/alcohol mixtures, but lost SABRE activity in more highly aqueous solvent mixtures. In the second strategy, diol functionalization of the COD ring provided a catalyst structure with lower water solubility, but sufficient to dissolve and activate in water to enable aqueous SABRE in a single step—without need for either an organic cosolvent or solvent removal followed by aqueous reconstitution—here demonstrated for the first time. The >30-fold ^{1}H enhancement under our conditions (with only 1 atm pH_2—a mere technical limitation of the bubbler apparatus used for those experiments) is in reasonable agreement with our recent observation of nearly 2000-fold enhancements of ^{1}H signals for the same substrate using the standard SABRE catalyst in deuterated methanol with elevated pH_2 pressures,[41] given the expected ~75-fold difference in pH_2 concentration; correspondingly, much larger enhancements should be expected upon implementing experimental approaches to greatly increase the pH_2 concentration, including higher-pressure reaction vessels. Moreover, the results presented here likely point the way to achieving higher aqueous catalyst concentrations, which should be possible by employing some combination of the above synthetic approaches (e.g., by functionalizing the COD with moieties that endow greater aqueous solubility). Such improvements, combined with other approaches, should help enable biological and spectroscopic applications that will be pursued in due course.

ASSOCIATED CONTENT

Supporting Information

The Supporting Information is available free of charge on the ACS Publications website at DOI: 10.1021/acs.jpcc.6b04484.

Details of the methods used to synthesize and characterize the catalysts, along with the details concerning the SABRE NMR experiments (PDF)

AUTHOR INFORMATION

Corresponding Author

*E-mail: bgoodson@chem.siu.edu. Phone: 618-453-6427.

Present Addresses

$^{\nabla}$F.S.: Advanced Imaging Research Center, University of Texas Southwestern Medical Center, Dallas, TX 75390.

$^{\bigcirc}$P.H.: Pennington Biomedical Research Center, Baton Rouge, LA 70808.

$^{\blacklozenge}$Q.B.: Department of Chemistry, Louisiana State University, Baton Rouge, LA 70803.

Author Contributions

¶F.S. and P.H. contributed equally.

Notes

The authors declare no competing financial interest.

ACKNOWLEDGMENTS

B.M.G. and F.S. thank Professor Jay Means (UCSB) for helpful discussions. Work at SIUC and Vanderbilt is supported by the NIH (1R21EB018014 and 1R21EB020323), NSF (CHE-1416432 and CHE-1416268), and DOD (CDMRP BRP W81XWH-12-1-0159/BC112431, and PRMRP awards W81XWH-15-1-0271 and W81XWH-15-1-0272). E.Y.C. also acknowledges support from Exxon Mobil Knowledge Build. A.M.C. also acknowledges support from NIH NIBIB T32 EB001628. F.S. gratefully acknowledges support from a Gower summer research fellowship (SIUC). B.M.G. is a member of SIUC Materials Technology Center.

REFERENCES

(1) Kurhanewicz, J.; Vigneron, D. B.; Brindle, K.; Chekmenev, E. Y.; Comment, A.; Cunningham, C. H.; DeBerardinis, R. J.; Green, G. G.; Leach, M. O.; Rajan, S. S.; et al. Analysis Of Cancer Metabolism By Imaging Hyperpolarized Nuclei: Prospects For Translation To Clinical Research. *Neoplasia* **2011**, *13*, 81−97.

(2) Weissleder, R. Molecular Imaging in Cancer. *Science* **2006**, *312*, 1168−1171.

(3) Nikolaou, P.; Goodson, B. M.; Chekmenev, E. Y. NMR Hyperpolarization Techniques for Biomedicine. *Chem.—Eur. J.* **2015**, *21*, 3156−3166.

(4) Ardenkjær-Larsen, J. H.; Fridlund, B.; Gram, A.; Hansson, G.; Hansson, L.; Lerche, M. H.; Servin, R.; Thaning, M.; Golman, K. Increase In Signal-To-Noise Ratio Of > 10,000 Times In Liquid-State NMR. *Proc. Natl. Acad. Sci. U. S. A.* **2003**, *100*, 10158−10163.

(5) Day, S. E.; Kettunen, M. I.; Gallagher, F. A.; Hu, D. E.; Lerche, M.; Wolber, J.; Golman, K.; Ardenkjaer-Larsen, J. H.; Brindle, K. M. Detecting Tumor Response To Treatment Using Hyperpolarized C-13 Magnetic Resonance Imaging And Spectroscopy. *Nat. Med.* **2007**, *13*, 1382−1387.

(6) Walker, T. G.; Happer, W. Spin-Exchange Optical Pumping Of Noble-Gas Nuclei. *Rev. Mod. Phys.* **1997**, *69*, 629−642.

(7) Goodson, B. M. Nuclear Magnetic Resonance of Laser-Polarized Noble Gases in Molecules, Materials, and Organisms. *J. Magn. Reson.* **2002**, *155*, 157−216.

(8) Bowers, C. R.; Weitekamp, D. P. Transformation Of Symmetrization Order To Nuclear-Spin Magnetization By Chemical-Reaction And Nuclear-Magnetic-Resonance. *Phys. Rev. Lett.* **1986**, *57*, 2645−2648.

(9) Eisenschmid, T. C.; Kirss, R. U.; Deutsch, P. P.; Hommeltoft, S. I.; Eisenberg, R.; Bargon, J.; Lawler, R. G.; Balch, A. L. Para Hydrogen Induced Polarization In Hydrogenation Reactions. *J. Am. Chem. Soc.* **1987**, *109*, 8089−8091.

(10) Mewis, R. E. Developments and Advances Concerning the Hyperpolarization Technique SABRE. *Magn. Reson. Chem.* **2015**, *53*, 789−800.

(11) Adams, R. W.; Aguilar, J. A.; Atkinson, K. D.; Cowley, M. J.; Elliott, P. I. P.; Duckett, S. B.; Green, G. G. R.; Khazal, I. G.; Lopez-Serrano, J.; Williamson, D. C. Reversible Interactions With Para-Hydrogen Enhance NMR Sensitivity By Polarization Transfer. *Science* **2009**, *323*, 1708−1711.

(12) Atkinson, K. D.; Cowley, M. J.; Elliott, P. P.; Duckett, S. B.; Green, G. G. R.; López-Serrano, J.; Whitwood, A. C. Spontaneous Transfer of Parahydrogen Derived Spin Order to Pyridine at Low Magnetic Field. *J. Am. Chem. Soc.* **2009**, *131*, 13362−13368.

(13) Bowers, C. R.; Weitekamp, D. P. Para-Hydrogen And Synthesis Allow Dramatically Enhanced Nuclear Alignment. *J. Am. Chem. Soc.* **1987**, *109*, 5541−5542.

(14) Haake, M.; Natterer, J.; Bargon, J. Efficient NMR Pulse Sequences to Transfer the Parahydrogen-Induced Polarization to Hetero Nuclei. *J. Am. Chem. Soc.* **1996**, *118*, 8688−8691.

(15) Bhattacharya, P.; Harris, K.; Lin, A. P.; Mansson, M.; Norton, V. A.; Perman, W. H.; Weitekamp, D. P.; Ross, B. D. Ultra-Fast Three Dimensional Imaging Of Hyperpolarized ^{13}C In Vivo. *MAGMA* **2005**, *18*, 245−56.

(16) Goldman, M.; Jóhannesson, H. Conversion Of A Proton Pair Para Order Into C-13 Polarization By RF Irradiation, For Use In MRI. *C. R. Phys.* **2005**, *6*, 575−581.

DOI: 10.1021/acs.jpcc.6b04484
J. Phys. Chem. C 2016, 120, 12149−12156

(17) Goldman, M.; Johannesson, H.; Axelsson, O.; Karlsson, M. Hyperpolarization Of C-13 Through Order Transfer From Para-hydrogen: A New Contrast Agent For MRI. *Magn. Reson. Imaging* **2005**, *23*, 153−157.
(18) Chekmenev, E. Y.; Hovener, J.; Norton, V. A.; Harris, K.; Batchelder, L. S.; Bhattacharya, P.; Ross, B. D.; Weitekamp, D. P. PASADENA Hyperpolarization Of Succinic Acid For MRI And NMR Spectroscopy. *J. Am. Chem. Soc.* **2008**, *130*, 4212−4213.
(19) Kovtunov, K. V.; Beck, I. E.; Bukhtiyarov, V. I.; Koptyug, I. V. Observation Of Parahydrogen-Induced Polarization In Heterogeneous Hydrogenation On Supported Metal Catalysts. *Angew. Chem., Int. Ed.* **2008**, *47*, 1492−1495.
(20) Eshuis, N.; van Weerdenburg, B. J. A.; Feiters, M. C.; Rutjes, F. P. J. T.; Wijmenga, S. S.; Tessari, M. Quantitative Trace Analysis of Complex Mixtures Using SABRE Hyperpolarization. *Angew. Chem., Int. Ed.* **2015**, *54*, 1372−1372.
(21) van Weerdenburg, B. J. A.; Glöggler, S.; Eshuis, N.; Engwerda, A. H. J. T.; Smits, J. M. M.; de Gelder, R.; Appelt, S.; Wymenga, S. S.; Tessari, M.; Feiters, M. C.; Blümich, B.; Rutjes, F. P. J. T. Ligand Effects of NHC−Iridium Catalysts for Signal Amplification by Reversible Exchange (SABRE). *Chem. Commun.* **2013**, *49*, 7388−7390.
(22) Ratajczyk, T.; Gutmann, T.; Bernatowicz, P.; Buntkowsky, G.; Frydel, J.; Fedorczyk, B. NMR Signal Enhancement by Effective SABRE Labeling of Oligopeptides. *Chem.—Eur. J.* **2015**, *21*, 12616−12619.
(23) van Weerdenburg, B. J.; Engwerda, A. H.; Eshuis, N.; Longo, A.; Banerjee, D.; Tessari, M.; Guerra, C. F.; Rutjes, F. P.; Bickelhaupt, F. M.; Feiters, M. C. Computational (DFT) and Experimental (EXAFS) Study of the Interaction of $[Ir(IMes)(H)_2(L)_3]$ with Substrates and Co-substrates Relevant for SABRE in Dilute Systems. *Chem.—Eur. J.* **2015**, *21*, 10482−10489.
(24) Barskiy, D. A.; Kovtunov, K. V.; Koptyug, I. V.; He, P.; Groome, K. A.; Best, Q. A.; Shi, F.; Goodson, B. M.; Shchepin, R. V.; Coffey, A. M.; et al. The Feasibility of Formation and Kinetics of NMR Signal Amplification by Reversible Exchange (SABRE) at High Magnetic Field (9.4 T). *J. Am. Chem. Soc.* **2014**, *136*, 3322−3325.
(25) Barskiy, D. A.; Kovtunov, K. V.; Koptyug, I. V.; He, P.; Groome, K. A.; Best, Q. A.; Shi, F.; Goodson, B. M.; Shchepin, R. V.; Truong, M. L.; et al. In Situ And Ex Situ Low-Field NMR Spectroscopy And MRI Endowed By SABRE Hyperpolarization. *ChemPhysChem* **2014**, *15*, 4100−4107.
(26) Daniele, V.; Legrand, F. X.; Berthault, P.; Dumez, J.-N.; Huber, G. Single-Scan Multidimensional NMR Analysis of Mixtures at Sub-Millimolar Concentrations by using SABRE Hyperpolarization. *ChemPhysChem* **2015**, *16*, 3413−3517.
(27) Pravdivtsev, A. N.; Yurkovskaya, A. V.; Vieth, H.-M.; Ivanov, K. L.; Kaptein, R. Level Anti-Crossings Are A Key Factor For Understanding Para-Hydrogen-Induced Hyperpolarization In SABRE Experiments. *ChemPhysChem* **2013**, *14*, 3327−3331.
(28) van Weerdenburg, B. J. A.; Eshuis, N.; Tessari, M.; Rutjes, F. P. J. T.; Feiters, M. C. Application of the π-Accepting Ability Parameter of N-heterocyclic Carbene Ligands in Iridium Complexes for Signal Amplification by Reversible Exchange (SABRE). *J. Chem. Soc., Dalton Trans.* **2015**, *44*, 15387−15390.
(29) Eshuis, N.; Hermkens, N.; van Weerdenburg, B. J.; Feiters, M. C.; Rutjes, F. P.; Wijmenga, S. S.; Tessari, M. Toward Nanomolar Detection by NMR Through SABRE Hyperpolarization. *J. Am. Chem. Soc.* **2014**, *136*, 2695−2698.
(30) Theis, T.; Truong, M. L.; Coffey, A. M.; Shchepin, R. V.; Waddell, K. W.; Shi, F.; Goodson, B. M.; Warren, W. S.; Chekmenev, E. Y. Microtesla SABRE Enables 10% Nitrogen-15 Nuclear Spin Polarization. *J. Am. Chem. Soc.* **2015**, *137*, 1404−1407.
(31) Moreno, K. X.; Nasr, K.; Milne, M.; Sherry, A. D.; Goux, W. J. Nuclear Spin Hyperpolarization of the Solvent Using Signal Amplification by Reversible Exchange (SABRE). *J. Magn. Reson.* **2015**, *257*, 15−23.
(32) Theis, T.; Truong, M. L.; Coffey, A. M.; Chekmenev, E. Y.; Warren, W. S. LIGHT-SABRE Enables Efficient In-Magnet Catalytic Hyperpolarization. *J. Magn. Reson.* **2014**, *248*, 23−26.
(33) Zeng, H.; Xu, J.; Gillen, J.; McMahon, M. T.; Artemov, D.; Tyburn, J.-M.; Lohman, J. A. B.; Mewis, R. E.; Atkinson, K. D.; Green, G. G. R.; et al. Optimization of SABRE for Polarization of the Tuberculosis Drugs Pyrazinamide and Isoniazid. *J. Magn. Reson.* **2013**, *237*, 73−78.
(34) Zeng, H.; Xu, J.; McMahon, M. T.; Lohman, J. A. B.; van Zijl, P. C. M. Achieving 1% NMR Polarization in Water in Less than 1 min. Using SABRE. *J. Magn. Reson.* **2014**, *246*, 119−121.
(35) Dücker, E. B.; Kuhn, L. T.; Münnemann, K.; Griesinger, C. Similarity Of SABRE Field Dependence In Chemically Different Substrates. *J. Magn. Reson.* **2012**, *214*, 159−165.
(36) Mewis, R. E.; Green, R. A.; Cockett, M. C.; Cowley, M. J.; Duckett, S. B.; Green, G. G.; John, R. O.; Rayner, P. J.; Williamson, D. C. Strategies for the Hyperpolarization of Acetonitrile and Related Ligands by SABRE. *J. Phys. Chem. B* **2015**, *119*, 1416−1424.
(37) Pravdivtsev, A. N.; Yurkovskaya, A. V.; Vieth, H.-M.; Ivanov, K. L. RF-SABRE: A Way to Continuous Spin Hyperpolarization at High Magnetic Fields. *J. Phys. Chem. B* **2015**, *119*, 13619−13629.
(38) Pravdivtsev, A. N.; Yurkovskaya, A. V.; Vieth, H.-M.; Ivanov, K. L. Spin Mixing at Level Anti-Crossings in the Rotating Frame Makes Hgh-Field SABRE Feasible. *Phys. Chem. Chem. Phys.* **2014**, *16*, 24672−24675.
(39) Pravdivtsev, A. N.; Yurkovskaya, A. V.; Zimmermann, H.; Vieth, H.-M.; Ivanov, K. L. Transfer of SABRE-Derived Hyperpolarization to Spin-1/2 Heteronuclei. *RSC Adv.* **2015**, *5*, 63615−63623.
(40) Glöggler, S.; Müller, R.; Colell, J.; Emondts, M.; Dabrowski, M.; Blümich, B.; Appelt, S. Para-Hydrogen Induced Polarization of Amino Acids, Peptides and Deuterium−Hydrogen Gas. *Phys. Chem. Chem. Phys.* **2011**, *13*, 13759−13764.
(41) Shi, F.; Porter, E.; Truong, M. L.; Coffey, A. M.; Waddell, K. W.; Chekmenev, E. Y.; Goodson, B. M. Interplay of Catalyst Structure and Temperature for NMR Signal Amplification by Reversible Exchange. Presented at the 56th Experimental Nuclear Magnetic Resonance Conference, Pacific Grove, CA, April 19−24, 2015.
(42) Fekete, M.; Bayfield, O.; Duckett, S. B.; Hart, S.; Mewis, R. E.; Pridmore, N.; Rayner, P. J.; Whitwood, A. Iridium(III) Hydrido N-Heterocyclic Carbene−Phosphine Complexes as Catalysts in Magnetization Transfer Reactions. *Inorg. Chem.* **2013**, *52*, 13453−13461.
(43) Appleby, K. M.; Mewis, R. E.; Olaru, A. M.; Green, G. G. R.; Fairlamb, I. J. S.; Duckett, S. B. Investigating Pyridazine and Phthalazine Exchange in a Series of Iridium Complexes in Order to Define Their Role in the Catalytic Transfer of Magnetisation from Para-Hydrogen. *Chem. Sci.* **2015**, *6*, 3981−3993.
(44) Ruddlesden, A. J.; Mewis, R. E.; Green, G. G.; Whitwood, A. C.; Duckett, S. B. Catalytic Transfer of Magnetism Using a Neutral Iridium Phenoxide Complex. *Organometallics* **2015**, *34*, 2997−3006.
(45) Fekete, M.; Gibard, C.; Dear, G. J.; Green, G. G.; Hooper, A. J.; Roberts, A. D.; Cisnetti, F.; Duckett, S. B. Utilisation of Water Soluble Iridium Catalysts for Signal Amplification by Reversible Exchange. *J. Chem. Soc., Dalton Trans.* **2015**, *44*, 7870−7880.
(46) Cowley, M. J.; Adams, R. W.; Atkinson, K. D.; Cockett, M. C.; Duckett, S. B.; Green, G. G.; Lohman, J. A.; Kerssebaum, R.; Kilgour, D.; Mewis, R. E. Iridium N-Heterocyclic Carbene Complexes As Efficient Catalysts For Magnetization Transfer From Para-Hydrogen. *J. Am. Chem. Soc.* **2011**, *133*, 6134−6137.
(47) Zhivonitko, V. V.; Skovpin, I. V.; Koptyug, I. V. Strong 31P Nuclear Spin Hyperpolarization Produced via Reversible Chemical Interaction with Parahydrogen. *Chem. Commun.* **2015**, *51*, 2506−2509.
(48) Truong, M. L.; Theis, T.; Coffey, A. M.; Shchepin, R. V.; Waddell, K. W.; Shi, F.; Goodson, B. M.; Warren, W. S.; Chekmenev, E. Y. ^{15}N Hyperpolarization By Reversible Exchange Using SABRE-SHEATH. *J. Phys. Chem. C* **2015**, *119*, 8786−8797.
(49) Shchepin, R. V.; Truong, M. L.; Theis, T.; Coffey, A. M.; Waddell, K. W.; Shi, F.; Warren, W. S.; Goodson, B. M.; Chekmenev, E. Y. NMR Signal Amplification by Reversible Exchange of Neat Liquids. *J. Phys. Chem. Lett.* **2015**, *6*, 1961−1967.
(50) Hövener, J.-B.; Schwaderlapp, N.; Borowiak, R.; Lickert, T.; Duckett, S. B.; Mewis, R. E.; Adams, R. W.; Burns, M. J.; Highton, L. A.; Green, G. G.; Olaru, A.; Hennig, J.; von Elverfeldt, D. Toward

DOI: 10.1021/acs.jpcc.6b04484
J. Phys. Chem. C 2016, 120, 12149−12156

Biocompatible Nuclear Hyperpolarization Using Signal Amplification By Reversible Exchange: Quantitative In Situ Spectroscopy And High-Field Imaging. *Anal. Chem.* **2014**, *86*, 1767−1774.
(51) Coffey, A. M.; Kovtunov, K. V.; Barskiy, D. A.; Koptyug, I. V.; Shchepin, R. V.; Waddell, K. W.; He, P.; Groome, K. A.; Best, Q. A.; Shi, F.; et al. High-Resolution Low-Field Molecular Magnetic Resonance Imaging Of Hyperpolarized Liquids. *Anal. Chem.* **2014**, *86*, 9042−9049.
(52) Lloyd, L. S.; Adams, R. W.; Bernstein, M.; Coombes, S.; Duckett, S. B.; Green, G. G. R.; Lewis, R. J.; Mewis, R. E.; Sleigh, C. J. Utilization of SABRE-Derived Hyperpolarization To Detect Low-Concentration Analytes via 1D and 2D NMR Methods. *J. Am. Chem. Soc.* **2012**, *134*, 12904−12907.
(53) Shi, F.; Coffey, A. M.; Waddell, K. W.; Chekmenev, E. Y.; Goodson, B. M. Heterogeneous Solution NMR Signal Amplification By Reversible Exchange. *Angew. Chem.* **2014**, *126*, 7625−7628.
(54) Shi, F.; Coffey, A. M.; Waddell, K. W.; Chekmenev, E. Y.; Goodson, B. M. Nanoscale Catalysts for NMR Signal Enhancement by Reversible Exchange. *J. Phys. Chem. C* **2015**, *119*, 7525−7533.
(55) Torres, O.; Martin, M.; Sola, E. Labile N-Heterocyclic Carbene Complexes Of Iridium. *Organometallics* **2009**, *28*, 863−870.
(56) Vazquez-Serrano, L. D.; Owens, B. T.; Buriak, J. M. The Search For New Hydrogenation Catalyst Motifs Based On N-Heterocyclic Carbene Ligands. *Inorg. Chim. Acta* **2006**, *359*, 2786−2797.
(57) Truong, M. L.; Shi, F.; He, P.; Yuan, B.; Plunkett, K. N.; Coffey, A. M.; Shchepin, R. V.; Barskiy, D. A.; Kovtunov, K. V.; Koptyug, I. V.; et al. Irreversible Catalyst Activation Enables Hyperpolarization And Water Solubility For NMR Signal Amplification By Reversible Exchange. *J. Phys. Chem. B* **2014**, *118*, 13882−13889.
(58) He, P.; Best, Q. A.; Groome, K. A.; Coffey, A. M.; Truong, M. L.; Waddell, K. W.; Chekmenev, E. Y.; Goodson, B. M. A Water-Soluble SABRE Catalyst for NMR/MRI Enhancement. Presented at the 55th Experimental Nuclear Magnetic Resonance Conference, Boston, MA, March 23−18, 2014.
(59) Shi, F.; Truong, M. L.; Coffey, A. M.; Shchepin, R.; Chekmenev, E. Y.; Goodson, B. M. Developments in NMR Signal Enhancement by Reversible Exchange (SABRE): Nanoscale Catalysts for HET-SABRE and a Water-Soluble Ir Catalyst for Aqueous SABRE in a Single Step. Presented at the 56th Experimental Nuclear Magnetic Resonance Conference, Pacific Grove, CA, April 19−24, 2015.
(60) Gallivan, J. P.; Jordan, J. P.; Grubbs, R. H. A Neutral, Water-Soluble Olefin Metathesis Catalyst Based on an N-Heterocyclic Carbene Ligand. *Tetrahedron Lett.* **2005**, *46*, 2577−2580.
(61) Purwanto; Deshpande, R. V.; Chaudhari, R. V.; Delmas, H. Solubility of Hydrogen, Carbon Monoxide, and 1-Octene in Various Solvents and Solvent Mixtures. *J. Chem. Eng. Data* **1996**, *41*, 1414−1417.
(62) Navon, G.; Song, Y. Q.; Room, T.; Appelt, S.; Taylor, R. E.; Pines, A. Enhancement of Solution NMR and MRI with Laser-Polarized Xenon. *Science* **1996**, *271*, 1848−1851.
(63) Pravdivtsev, A. N.; Ivanov, K. L.; Yurkovskaya, A. V.; Petrov, P. A.; Limbach, H. H.; Kaptein, R.; Vieth, H.-M. Spin Polarization Transfer Mechanisms of SABRE: A Magnetic Field Dependent Study. *J. Magn. Reson.* **2015**, *261*, 73−82.
(64) Shchepin, R. V.; Barskiy, D. A.; Coffey, A. M.; Theis, T.; Shi, F.; Warren, W. S.; Goodson, B. M.; Chekmenev, E. Y. ^{15}N Hyperpolarization of Imidazole-$^{15}N_2$ for Magnetic Resonance pH Sensing via SABRE-SHEATH. *ACS Sensors* **2016**, DOI: 10.1021/acssensors.6b00231.
(65) Shchepin, R. V.; Barskiy, D. A.; Mikhaylov, D. M.; Chekmenev, E. Y. Efficient Synthesis of Nicotinamide-1−^{15}N for Ultrafast NMR Hyperpolarization Using Parahydrogen. *Bioconjugate Chem.* **2016**, *27*, 878−882.
(66) Spannring, P.; Reile, I.; Emondts, M.; Schleker, P.; Hermkens, N.; van der Zwaluw, N.; van Weerdenburg, B.; Tinnemans, P.; Tessari, M.; Blumich, B.; Rutjes, F.; Feiters, M. Development and Application of a Water Soluble SABRE Catalyst. Presented at the 57th Experimental Nuclear Magnetic Resonance Conference, Pittsburgh, PA, April 10−16, 2016.

NOTE ADDED IN PROOF

Readers may also be interested to note the very recent presentation of Philipp Schleker and co-workers, who reported the preparation and application of a different water-soluble Ir-based SABRE catalyst.[66]

DOI: 10.1021/acs.jpcc.6b04484
J. Phys. Chem. C 2016, 120, 12149−12156